MOLECULAR AND CELLULAR BIOLOGY, Apr. 2007, p. 2758–2764 Vol. 27, No. 7
0270-7306/07/$08.00+0 doi:10.1128/MCB.02334-06

Developmental Changes in Histone macroH2A1-Mediated Gene Regulation▽†

Lakshmi N. Changolkar, Carl Costanzi, N. Adrian Leu, Dannee Chen, K. John McLaughlin, and John R. Pehrson*

Department of Animal Biology, School of Veterinary Medicine, University of Pennsylvania, Philadelphia, Pennsylvania 19104

Received 14 December 2006/Accepted 5 January 2007

macroH2A histone variants have been implicated to function in gene silencing by several studies, including ones showing a preferential association of macroH2A on the inactive X chromosome. To examine macroH2A function in vivo, we knocked out *macroH2A1*. *macroH2A1* knockout mice are viable and fertile. A broad screen of liver gene expression showed no evidence of defects in X inactivation but did identify genes that have increased expression levels in *macroH2A1* knockouts. macroH2A1-containing nucleosomes are enriched on the coding and/or upstream regions of these genes, suggesting that their increased expression levels are a direct effect of the absence of macroH2A1. The concentrations of macroH2A1 nucleosomes on these genes are low in the livers of newborn mice, and the *macroH2A1* knockout had little effect on the expression levels of these genes in newborn liver. Our results indicate that an increase in liver macroH2A1 during the transition from newborn to young-adult status contributes to a decrease in the expression levels of these genes. These genes cluster in the area of lipid metabolism, and we observed metabolic effects in *macroH2A1* knockouts. Our results indicate that the function of macroH2A1 histones is not restricted to gene silencing but also involves fine tuning the expression of specific genes.

The nucleosome is an important target for modifying chromatin functions, including transcription. One mechanism for modifying nucleosome function is the substitution of variant histones for the major or canonical histones. Genetic studies showed that histone variants H2A.X, H2A.Z, CENPA, and H3.3 have important functional properties that cannot be provided by their conventional counterparts (reviewed in reference 24).

macroH2A histone variants have an unusual structure, consisting of a full-length H2A domain linked to a large nonhistone domain, producing proteins that are nearly three times the size of conventional core histones (Fig. 1A) (26). macroH2As are highly conserved among vertebrates (1, 27). They appear to be absent from most invertebrates but are present in the sea urchin. The H2A domain of macroH2As is ~65% identical to conventional H2As. Most of the nonhistone region appears to be derived from a domain that is found in many contexts (3, 27). Recent studies showed that some "macrodomains," including the one from macroH2A1.1, bind ADP ribose (17). The significance of this binding for macroH2A function is not known. There are three macroH2A variants. macroH2A1.1 and 1.2 are formed by alternate splicing of *macroH2A1* (gene symbol *H2afy*), while macroH2A2 is encoded by a separate gene (4, 7, 26, 30). The distributions of macroH2A variants are different in different cell types and change during development (7, 25). The macroH2A1 (1.1 and 1.2) content of adult rat liver chromatin, a relatively rich source of macroH2A1, was estimated to be one for every 30 nucleosomes (26).

The distribution of macroH2A in chromatin suggests a role in transcriptional repression. We recently mapped the distribution of macroH2A1, using DNA isolated from macroH2A1-containing nucleosomes (5). Active genes were depleted of macroH2A1, while the inactive X chromosome showed preferential enrichment. macroH2A1 was not enriched on four regions of the inactive X chromosome that escape inactivation (5). The enrichment of macroH2A on the inactive X chromosome was previously observed by immunofluorescence and by expression of macroH2A-green fluorescent protein fusion proteins (4, 6–8). A recent study showed that a macroH2A1 knockdown decreases the stability of X inactivation in cultured human cells, indicating that macroH2A1 has a role in maintenance of X inactivation (15). Immunofluorescence studies indicate that macroH2As are preferentially associated with other large domains of the transcriptional silent chromatin, including pericentromeric heterochromatin in some cell types (8, 11), the XY body of spermatocytes (16), and transcriptionally silent senescence-associated heterochromatic foci (36). A role for macroH2A1 in gene silencing is supported by a recent study that showed a dramatic derepression of interleukin-8 (IL-8) when macroH2A1 expression was knocked down in a cultured human B-cell line (2). In this paper, we investigate the in vivo functions of macroH2A by examining the effects of a *macroH2A1* knockout mutation on gene expression in mouse liver.

MATERIALS AND METHODS

Mice. All animal protocols were approved by the University of Pennsylvania Institutional Animal Care and Use Committee. Mice were maintained on a 12-h day/night cycle, with the lights coming on at 8 a.m. Mice used for organ harvest were killed between 8 and 11 a.m. For most studies, *macroH2A1* knockout mice and their age- and sex-matched controls were raised in the same cage.

* Corresponding author. Mailing address: Department of Animal Biology, School of Veterinary Medicine, University of Pennsylvania, Philadelphia, PA 19104. Phone: (215) 898-0454. Fax: (215) 573-5189. E-mail: pehrson@vet.upenn.edu.

† Supplemental material for this article may be found at http://mcb.asm.org/.

▽ Published ahead of print on 22 January 2007.

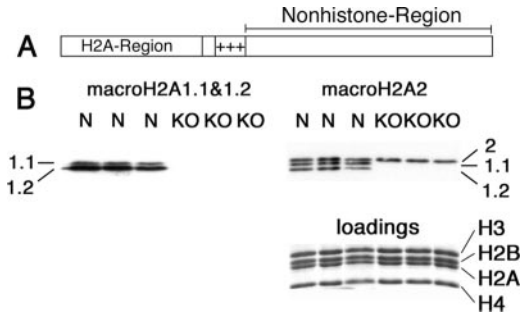

FIG. 1. Absence of macroH2A1 proteins in the *macroH2A1* knockout. (A) Diagram of macroH2A. The H2A region is ~65% identical to conventional H2A. +++ indicates a highly basic region that may bind DNA. macroH2A1.1 and 1.2 differ in a single ~30-amino-acid segment in the nonhistone region. (B) Western blots with antibodies against nonhistone regions of macroH2A1.1 and 1.2 (left) and macroH2A2 (right) are shown; note that this macroH2A2 serum has some cross-reaction with macroH2A1.1 and 1.2, so all three macroH2A variants show. macroH2A1 variants are much more abundant in mouse liver than macroH2A2 (7). Total nuclear extracts were prepared from normal mouse liver (lanes N) and *macroH2A1* knockout mouse liver (lanes KO). Loadings were equalized using core histones (see stained gel below the macroH2A2 blot).

***macroH2A1* knockout.** We based the targeting vector on an ~10-kb ApaI fragment of mouse genomic DNA that contains exon 2 of *macroH2A1* (*H2afy*) (see Fig. S1 in the supplemental material). We obtained this fragment from a mouse bacterial artificial chromosome clone (library CitbCJ7; Invitrogen) made from an embryonic stem (ES) cell line that has a 129Sv background. A cassette containing a promoterless internal ribosome entry site βgeo marker (22) was inserted into a PstI site in the first intron. This cassette was flanked by *LoxP* sites. A third *LoxP* site was inserted into a SalI site in the second intron (see Fig. S1 in the supplemental material).

Electroporation and drug selection were done by Incyte Genomics Inc., using 129SvJ ES cells. G418-resistant clones were screened by Southern blot analyses, with genomic fragments just 5′ or 3′ of the ApaI fragment used for the targeting vector (see Fig. S1 in the supplemental material). A clone that was positive for homologous recombination was transiently transfected with a plasmid that expressed the Cre recombinase (pMCCreN) (12), and G418-sensitive clones were screened by PCR for excision of the internal ribosome entry site βgeo cassette and exon 2.

ES cells were injected into C57BL/6 blastocysts, and the chimeric males were mated to obtain germ line transmission of the *macroH2A1* knockout allele. The *macroH2A1* knockout allele was backcrossed into the C57BL/6 background for 10 generations. *macroH2A1* knockout and normal alleles were identified by PCR (see Fig. S1 in the supplemental material), using a small piece of the tail that was digested with proteinase K. The primers used were as follows: Pst forward, GTGAGACACTTGAGAAAAGTCATTGTCAGTATAAC; Pst reverse, AACAGCACAGCAGGCAGCTGCTGA; Sal reverse, CCTCCAGTCCTTGTTCAACATAACCACCAT. Reactions were run using *Taq* polymerase from New England Biolabs in its standard buffer with an annealing temperature of 55°C.

Microarrays. The mice were raised in the same cage following weaning and were all killed over a period of approximately 1 h on the same morning. The large lobe of the liver was immediately dissected and frozen in liquid nitrogen. Total RNA was isolated using TRIzol (Invitrogen). RNA concentration was estimated by UV absorption and confirmed by gel electrophoresis.

All protocols were conducted as described in the Affymetrix GeneChip expression analysis technical manual. Briefly, total RNA was converted to first-strand cDNA using Superscript II reverse transcriptase primed by a poly(T) oligomer that incorporated the T7 promoter. Second-strand cDNA synthesis was followed by in vitro transcription for linear amplification of each transcript and incorporation of biotinylated CTP and UTP. The cRNA products were fragmented to 200 nucleotides or less, heated at 99°C for 5 min, and hybridized for 16 h at 45°C to Affymetrix MOE430 v2.0 microarrays. The microarrays were then washed at low (6× SSPE) (1× SSPE is 0.18 M NaCl, 10 mM NaH_2PO_4, and 1 mM EDTA [pH 7.7]) and high (100 mM MES [morpholineethanesulfonic acid], 0.1 M NaCl) stringencies and stained with streptavidin-phycoerythrin. Fluorescence was amplified by adding biotinylated anti-streptavidin and an additional aliquot of streptavidin-phycoerythrin stain. A confocal scanner was used to collect fluorescence signal after excitation at 570 nm.

Affymetrix Microarray Suite 5.0 was used to quantitate expression levels for targeted genes; default values provided by Affymetrix were applied to all analysis parameters. Border pixels were removed, and the average intensity of pixels within the 75th percentile was computed for each probe. The average of the lowest 2% of probe intensities occurring in each of 16 microarray sectors was set as the background and subtracted from all features in that sector. Probe intensities were then exported as .cel files and imported into GeneSpring (v7.2; Agilent Technologies), where probe set signals were calculated using Gene Chip robust multiarray. The expression values were $\log_2$ transformed in Excel and analyzed using statistical analysis of microarrays (SAM v2.1; Stanford University). This analysis gave us a list of the 111 most significant genes (see Table S1 in the supplemental material). This list had a maximum false-discovery rate of 47% based on 200 permutations.

Subtractive hybridization. We used PCR Select subtractive hybridization (Clontech Laboratories, Palo Alto, CA) to enrich for cDNAs with increased abundance in cDNA prepared from female *macroH2A1* knockout liver in comparison to that for normal female mouse liver. Subtracted cDNA was cloned, and clones that were enriched in the subtracted cDNA were sequenced and tested by real-time PCR for enrichment in unsubtracted *macroH2A1* knockout liver cDNA.

Real-time PCR. Real-time PCR was performed using the LightCycler system (Roche Applied Science). We used Titanium *Taq* polymerase (BD Biosciences) with its standard buffer. Denaturation was for 1 s at 95°C, annealing for 3 s (variable temperatures) (see Table S3 in the supplemental material), and elongation for 5 s at 72°C for reactions with genomic DNA and 13 s at 72°C for reactions with cDNA. Detection was with SYBR green I, and quantification was done with standard LightCycler data analysis software, using the second derivative maximum to compare different samples. Using three standard primer pairs, we estimated a difference of approximately 1.9-fold per cycle and used this value for all primer pairs. Product purity was checked by melting curves and gel electrophoresis. We synthesized cDNA, using poly $d(T)_{12-18}$ (Amersham Biosciences) as a primer and BD PowerScript reverse transcriptase (CloneTech) under standard conditions. All cDNAs were normalized using primers to glyceraldehyde phosphate dehydrogenase. Following normalization, normal and knockout cDNA samples were compared directly in the same run. Genomic DNAs were equalized by UV absorption and by ethidium bromide-stained agarose gels. Primer sequences are listed in Table S3 in the supplemental material.

Glucose tolerance test. Mice were fasted overnight and the following morning were injected with 2 g glucose/kg of body weight intraperitoneally, using a solution of 20% glucose dissolved in phosphate-buffered saline. Blood glucose was measured at 0, 15, 30, 60, 90, and 120 min following the injection, using a One Touch Ultra glucometer. Blood was collected by cutting the tip of the tail. The mice were 2 to 3.5 months of age. Knockout and normal mice used in individual tests were closely age matched, usually within a week, and knockout and normal mice were caged together in most cases. We tested 63 different normal males, 49 knockout males, 44 normal females, and 47 knockout females. There was no difference in the average weights of knockout and normal males. The average weight of the knockout females was slightly higher than that for the normal females, 21.4 versus 20.7 g.

Purification of macroH2A1-containing nucleosomes. macroH2A1-containing mono- and oligonucleosomes were purified from bulk chromatin by thiol affinity chromatography as described previously (5). Briefly, an H1-stripped S2 chromatin fraction was digested to mono- and oligonucleosomes and macroH2A1-containing nucleosomes were purified by binding them to thiopropyl Sepharose (Amersham Biosciences) and eluting them with mercaptoethanol. The chromatin was passed through a column of activated thiol Sepharose (Amersham Biosciences), which does not preferentially bind macroH2A1, prior to being passed through a thiopropyl Sepharose column. The thiopropyl column was washed with 0.5 M NaCl to remove nucleosomes bound by nonhistone proteins prior to elution of macroH2A1-containing nucleosomes with mercaptoethanol.

Northern blots. RNA was run in formaldehyde-containing 1% agarose gels (NorthernMax; Ambion) under standard conditions. The transfers were done by downward elution with 5× SSC (1× SSC is 0.15 M NaCl plus 0.015 M sodium citrate)/10 mM NaOH (following the Ambion protocol) onto Zeta-Probe GT membranes (Bio-Rad). Membranes were washed in 2× SSC and UV cross-linked. Hybridization was done at 65°C, following the standard protocol for Zeta-Probe GT membranes. The *Lpl* probe was the insert from a mouse cDNA clone (gi 13097035). The *Serpina7* probe was prepared by PCR amplification from mouse liver cDNA. The primers were as follows: forward, GTATCGGAGGCTCTCTGTGG; reverse, GGAGGTACTTCCTGCTGATCC. The product

is 981 bp based on *Serpina7* cDNA sequences. DNA probes were labeled by random priming.

Western blot analysis. Proteins were separated by sodium dodecyl sulfate gel electrophoresis, transferred onto polyvinylidene difluoride membranes (7, 25), and probed with rabbit polyclonal antibodies raised against the nonhistone regions of rat macroH2A1.1, 1.2, and 2 (6). The blocked membranes were incubated overnight with the primary antibody, followed by a secondary peroxidase conjugated donkey anti-rabbit immunoglobulin G, and the signal was detected using chemiluminescence.

RESULTS

Knockout of *macroH2A1*. We produced a knockout mutation of *macroH2A1* by removing the second exon (see Fig. S1 in the supplemental material). This exon contains the initiation codon and encodes the first part of the H2A domain. The next methionine does not occur until the final 30 amino acids of the protein, making it very unlikely that any functional macroH2A-like protein could be encoded by the knockout allele. Western blot analysis confirmed that neither macroH2A1.1 nor macroH2A1.2 was present in nuclear extracts prepared from the livers of *macroH2A1* knockout mice (Fig. 1B).

macroH2A1 knockout mice develop and grow with no obvious defects in their appearances, sizes, or fertility. The fertility of males suggests that macroH2A1 is not required for silencing of the XY body, although we have not directly addressed this question. We have not observed any obvious deficiency in the births of *macroH2A1* knockout males or females. The viability of knockout females rules out any gross deficiency in X inactivation (21). We kept eight *macroH2A1* knockout and eight control females for more than 1.5 years without the emergence of any consistent unusual pathology in the knockouts. Histological analysis of three knockout females showed no significant pathology at 8 weeks of age. In comparison to age-matched controls, the knockouts had mildly enlarged spleens, increased lymphocytic inflammation in a variety of tissues, and smaller Peyer's patches, but these differences were within normal limits.

We examined the possibility of up-regulation of macroH2A2 in *macroH2A1* knockout mice by Western blot analyses (Fig. 1B). Scans of the Western blot did not detect a change in the overall level of macroH2A2 in the livers of *macroH2A1* knockout mice. Immunofluorescence studies of *macroH2A1* knockout liver did not reveal any obvious increase in the macroH2A2 content of hepatocytes (not shown). As expected, the immunofluorescence for macroH2A1, including staining of the inactive X chromosome, was lost in *macroH2A1* knockout liver (not shown).

Gene expression in *macroH2A1* knockout liver. We used an Affymetrix MOE 430 v2.0 microarray to compare gene expression in *macroH2A1* knockout liver to that in normal mouse liver. This array is based on the mouse UniGene database (build 107, June 2002) and was designed to probe the expression of more than 34,000 genes. The knockout mutation was inbred into the C57BL/6 background for 10 generations. Normal and knockout mice were caged together, and livers were collected at the same time of day; the mice were 2-month-old females. Livers from five normal mice were compared to livers from five *macroH2A1* knockouts. We used significance analysis of microarrays (SAM v2.1; Stanford University) to analyze the results (32). With the maximum false-discovery rate set at 47%, significance analysis of microarrays identified 54 genes that had increased expression levels in *macroH2A1* knockout liver and 50 genes that had decreased expression levels (see Table S1 in the supplemental material). Most of these genes showed <2-fold changes.

TABLE 1. Expression of selected genes in *macroH2A1* knockout mice

Gene	Value for indicated liver group			Function	Reference
	Adult[a]		Newborn female[b,c]		
	Female[c]	Male[c]			
Serpina7	4.1[f]	1.8[f]	0.76[g]	Serum thyroxine binding protein	31
Lpl	2.6[f]	2.6[f]	1.1[d]	Hydrolysis of circulating triacylglycerols	29
Krt1-23	2.4[f]	5.6[f]	1.1	Type 1 keratin	35
ATP11a	1.9[f]	1.5[d]	1.1	Putative transbilayer amphipath transporter	13
Scd2	1.5[d]	1.4[d]	1.1	Fatty acid desaturase	23
CD36	1.4[e]	1.6[f]	1.0	Fatty acid translocase	28
Thrsp	1	1.6[e]	ND	Regulates fatty acid synthesis	37
GTPbp4	0.78[e]	0.9	ND	Nuclear GTP binding protein	20
Sucnr1	0.77[d]	1.1	ND	G protein couple receptor for succinate	14
Ar	0.65[d]	1.2	ND	Androgen-regulated transcription factor	33

[a] Numbers of adult livers: female, 13 normal and 12 knockout; male, 12 normal and 12 knockout.
[b] Numbers of newborn female (3-day) livers: seven normal and eight knockout. Similar results were obtained with a smaller group of newborn males.
[c] Values were determined in duplicate by real-time PCR and are given as ratios of expression levels for *macroH2A1* knockout mice to those for normal controls. ND, not determined.
[d] $P < 0.05$ (one-tailed t test).
[e] $P < 0.01$ (one-tailed t test).
[f] $P < 10^{-4}$ (one-tailed t test).
[g] $P < 0.05$ (two-tailed t test).

There is no evidence for reactivation of the inactive X chromosome in this microarray analysis. Only 3 of the 54 genes that showed increased expression levels are on the X chromosome, and 1 of these, *Dlgh3*, did not show increased expression levels when we analyzed it by real-time PCR in a larger group of females. The absence of any obvious effect on X inactivation is consistent with previous studies that showed that X inactivation is robustly maintained by multiple mechanisms (9, 15).

In order to identify genes that have consistently altered expression levels in *macroH2A1* knockout mice, we used real-time PCR to examine the expression of selected genes in the livers of a large independent group of 2-month-old females. This analysis identified five genes that have significantly increased expression levels in the knockouts (Table 1). We used Northern blot analysis to examine the expression of two of these genes, the lipoprotein lipase (*Lpl*) and thyroxine binding globulin (*Serpina7*) genes. This analysis confirmed the PCR results and gave no evidence of unusual transcripts in the knockout mice (Fig. 2). Our PCR analysis identified three genes that showed small but significant decreases in expression in *macroH2A1* knockout liver (Table 1).

The five genes that were significantly increased in female knockouts also had increased expression levels in male knockout liver (Table 1). There were two notable differences. One was *Serpina7*, which was 1.8-fold higher in knockout males

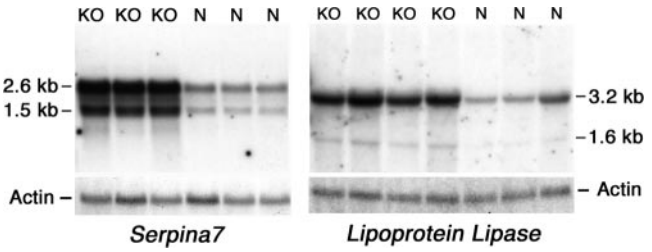

FIG. 2. Northern blot analysis of *Serpina7* and *Lpl* expression in *macroH2A1* knockout mice. Total mouse liver RNA was analyzed on Northern blots for *Serpina7* and *Lpl* expression. The blots were rehybridized with β actin to show equal loadings. KO, RNA from female *macroH2A1* knockout mouse liver; N, RNA from normal female mouse liver.

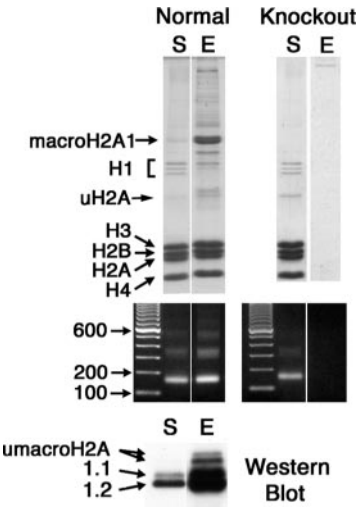

FIG. 3. Purification of macroH2A1-containing nucleosomes by thiol-affinity chromatography. Mouse liver mono- and oligonucleosomes were prepared, and macroH2A1-containing chromatin fragments were purified by selective thiol affinity chromatography (5). S, starting material; E, material eluted from thiopropyl Sepharose with β-mercaptoethanol. The mercaptoethanol-eluted chromatin is highly enriched for macroH2A1-containing nucleosomes. Results for normal mouse liver are shown on the left, and results for *macroH2A1* knockout liver are on the right. Protein compositions were analyzed by sodium dodecyl sulfate gel electrophoresis (top panels). DNA was analyzed in agarose gels (middle panels). The bottom panel is a Western blot of the starting material and a pool of the eluted fractions stained with antibodies against macroH2A1.1 and 1.2; these lanes were loaded for equal amounts of H3 and H4.

compared to more than 4-fold higher in knockout females. The other was *Krt1-23*, which was 5.6-fold higher in knockout males compared to 2.4-fold higher in knockout females. In contrast to those in female liver, expression levels of *Ar*, *Sucnr1*, and *GTPbp4* were not significantly decreased in male knockout liver. The sexual dimorphic effect of the knockout on *Serpina7* expression may be related to the sexual dimorphic expression of this gene in normal mice, which we found to be nearly four times higher in normal adult males than in normal adult females. *Krt1-23* expression levels were about 30% higher in normal adult females than in normal adult males.

We identified two additional genes that have increased expression levels in *macroH2A1* knockout mice. The thyroid hormone responsive SPOT14 homolog gene (*Thrsp*) was identified in a microarray analysis of gene expression in male *macroH2A1* knockout liver, and *CD36* was identified by subtractive hybridization. Both of these genes were confirmed by real-time PCR, but *Thrsp* showed increased expression levels only in males (Table 1). Interestingly, four of the seven genes that have increased expression levels in knockouts encode proteins directly involved in fatty acid metabolism (Table 1).

Distribution of macroH2A1 on genes with altered expression levels. We examined the distribution of macroH2A1-containing nucleosomes on the genes that had altered expression levels in order to assess whether the effect of the knockout on these genes was likely to be direct. We purified macroH2A1-containing mono- and oligonucleosomes with a high degree of specificity, using our previously described thiol affinity procedure (Fig. 3) (5). We used real-time PCR to compare the distribution of specific sequences in DNA isolated from macroH2A1-containing nucleosomes to that in DNA from the nucleosomes applied to the columns. The results presented in Fig. 4 are the averages for four preparations, two from male liver and two from female liver. The male and female results are presented separately in Table S2 in the supplemental material and in most cases were very similar to each other.

macroH2A1 was enriched on the transcribed and upstream regions of *Scd2*, *Krt1-23*, and *Serpina7* (Fig. 4, adult liver), consistent with the possibility that the increased expression levels of these genes in knockouts are a direct effect of the absence of macroH2A1. *Serpina7* is located on the X chromosome. In contrast to what we have seen with other active X-linked genes (5), *Serpina7* showed nearly equal enrichment levels for macroH2A1 in male samples and female samples at most sites (see Table S2 in the supplemental material). macroH2A1 was enriched on the upstream regions of *Lpl* and *ATP11a* (Fig. 4, adult liver). This suggests that the increased expression levels of these genes in *macroH2A1* knockout liver may be a direct effect of the knockout on the regulatory regions of these genes. This enrichment was especially striking for *Lpl*, where it started within 450 bp of the start of the gene and extended to more than 10 kb upstream. macroH2A1 was depleted on most of the transcribed regions that we probed for both of these genes, consistent with what we have observed for other active genes (5).

We examined the distribution of macroH2A1 on two of the genes that had decreased expression levels in female *macroH2A1* knockout liver (Fig. 4). As with most active genes that we have examined, macroH2A1 was depleted on the transcribed and nearby upstream regions of *GTPbp4*. There was a small enrichment for macroH2A1 on both the transcribed and the upstream regions of *Sucnr1*. The low concentrations of macroH2A1 on these genes indicate that the effect of a *macroH2A1* knockout on these genes is indirect.

Gene expression in newborn liver. The macroH2A1 content of liver nuclei from 3-day-old mice is much lower than that of liver nuclei from 2-month-old mice (Fig. 5) (25). Based on scans of Western blots, the macroH2A1.1 content of liver nuclei isolated from 3-day-old-mice was 16-fold lower and the macroH2A1.2 content was 2.7-fold lower. This suggested that the effect of a *macroH2A1* knockout on gene expression might be different in the livers of newborn mice. Indeed, none of the

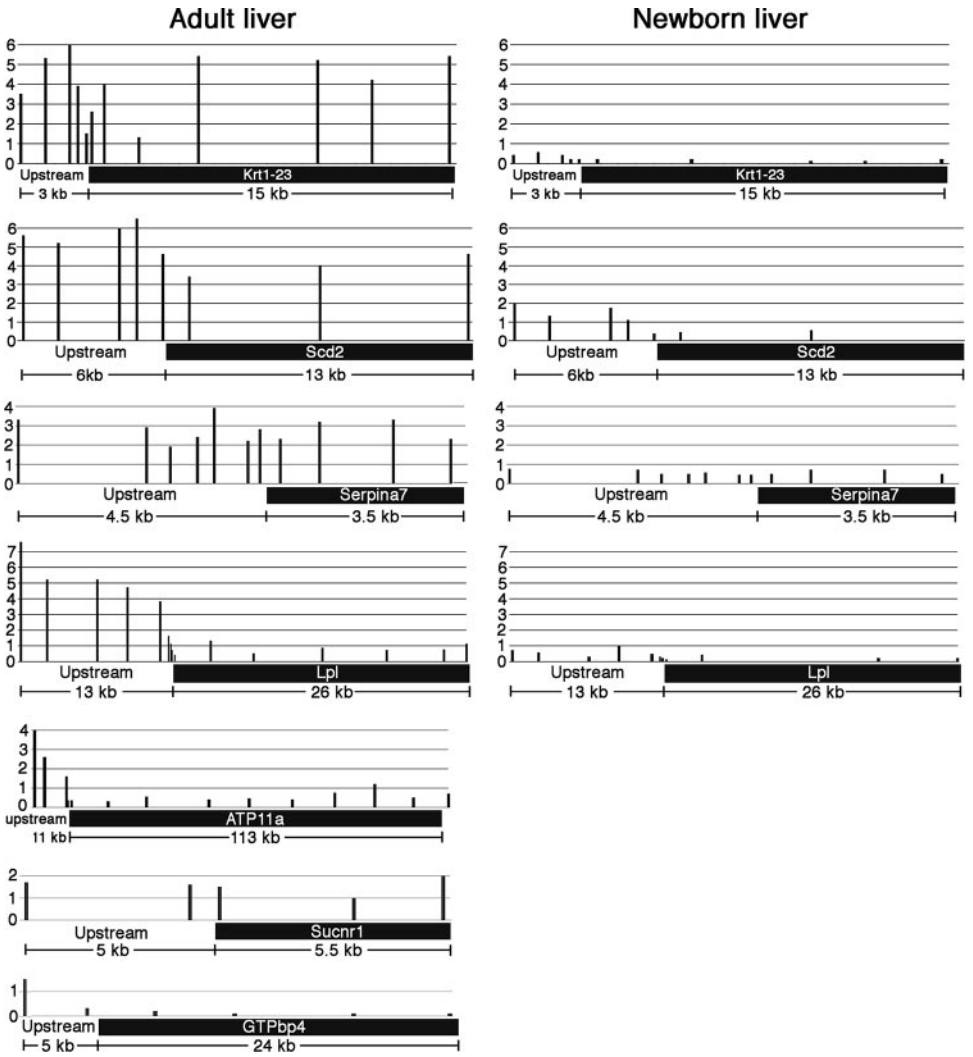

FIG. 4. Distribution of macroH2A1 on genes that have altered expression levels in *macroH2A1* knockout mouse liver. Results for adult liver (2-month-old mice) are on the left, and those for newborn liver (3-day-old mice) are on the right. macroH2A1-containing chromatin fragments were purified from normal mouse liver (Fig. 3). The relative macroH2A1 concentration on a sequence was estimated by using real-time PCR to calculate the relative concentration of the sequence in the macroH2A1-enriched, thiopropyl-eluted fraction in comparison to that of the starting material. A value of 1 on the scales on the left of the diagrams indicates a macroH2A1 concentration equal to that of the starting material prepared from adult liver. A few sites tested with the genes of the adult samples were not tested with the newborn samples. The horizontal bars on the bottom of the charts indicate the transcribed regions of the genes.

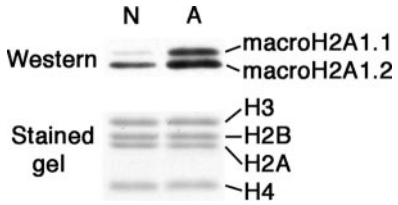

FIG. 5. Developmental changes in the macroH2A1 content of mouse liver nuclei. Nuclei were isolated from the livers of newborn (3-day-old) and adult (2-month-old) mice. Total nuclear extracts were analyzed on Western blots using antibodies against macroH2A1.1 and 1.2. Gels were loaded for equal content of core histones; see Coomassie blue-stained lanes below the blot. Lane N, extract from newborn livers; lane A, extract from adult livers.

genes that showed increased expression levels in adult knockout liver showed increased expression levels in newborn knockout liver (Table 1). The expression levels of *Serpina7*, *Lpl*, *Scd2*, *Krt1-23*, and *CD36* are higher in newborn liver than in adult liver, but *ATP11a* expression levels were similar in newborn and adult livers (Table 2). These findings suggest that an increase in liver macroH2A1 during this period contributes in part to a decrease in the expression levels of *Serpina7*, *Lpl*, *Scd2*, *Krt1-23*, and *CD36*. Consistent with this idea, we found that the concentrations of macroH2A1 on *Serpina7*, *Lpl*, *Scd2*, and *Krt1-23* were much lower in the livers of newborn mice than in adult livers (Fig. 4).

Glucose metabolism. Lipoprotein lipase hydrolyzes triacylglycerols circulating in lipoprotein complexes in the blood and has a crucial role in the delivery of fatty acids to the tissues (29). It is expressed in neonatal mouse liver, but its expression

TABLE 2. Expression in newborn and adult livers

Gene	Expression level[a]
Serpina7	20
Lpl	12.5
Krt1-23	17.9
Scd2	5.9
ATP11a	1
CD36	2.2

[a] Expression levels in six newborn and six adult females were determined by real-time PCR and were normalized to glyceraldehyde phosphate dehydrogenase expression levels.

levels in adult mouse liver are low (29). Mice that carry a liver-specific *Lpl* transgene that increases liver lipoprotein lipase expression levels fourfold develop insulin resistance in the liver and reduced glucose tolerance secondary to the increased delivery of fatty acids to the liver (18). The livers of adult *macroH2A1* knockouts have increased expression levels of *Lpl* and the fatty acid transporter *CD36*, which should lead to increased fatty acid delivery and reduced glucose tolerance. As expected, *macroH2A1* knockout males had significantly higher concentrations of blood glucose in glucose tolerance tests at all times except zero time (Fig. 6). Female knockouts showed only a small increase in blood glucose at the 30-min time point. We believe that this sexual dimorphism may reflect a difference in the responses of females and males to increased delivery of fatty acids to the liver. Previous studies of the effects of increased fatty acid delivery on liver insulin resistance have been done on male mice and rats (18, 19, 34), suggesting that the responses of females may be different.

DISCUSSION

macroH2A histone variants have been implicated to function in gene silencing. Interestingly, our broad-based examination of gene expression in *macroH2A1* knockout mouse liver did not discover any genes showing dramatic derepression. Instead, we discovered several genes that showed moderate but consistent increases in expression. macroH2A1-containing nucleosomes were preferentially present in the upstream and/or transcribed regions of these genes, indicating that macroH2A1 in the regulatory and/or transcribed regions of these genes has a direct repressive effect on their expression levels. The distribution of macroH2A1 that we observed did not provide evidence for the localization of macroH2A1 to a particular site or small region of these genes. Instead, we found relatively large domains of similar macroH2A1 enrichment in the upstream and/or transcribed regions. We believe that these domains exert a repressive effect on these genes. The case for a direct effect on *ATP11a* is weaker, because the domain of macroH2A1 enrichment begins rather far upstream. Recent studies using in vitro transcription indicate that macroH2A1.2 nucleosomes can directly inhibit initiation of transcription (10). It is not known how close they need to be to the promoter region to exert a repressive effect or whether their presence on transcribed regions inhibits elongation. We discovered a few genes that have reduced expression levels in *macroH2A1* knockout mice. macroH2A1 nucleosomes showed little or no enrichment on these genes, suggesting that their reduced expression levels are an indirect effect of the knockout.

Four of the seven genes that we identified as having increased expression levels in *macroH2A1* knockouts are directly involved in fatty acid metabolism: *Lpl*, *Scd2*, *Thrsp*, and *CD36* (Table 1). This suggests that macroH2A1-mediated regulation of gene expression may be a mechanism for bringing about coordinated adaptive changes to the metabolic state of liver cells. Our studies with newborn and young-adult mouse liver support this idea. There is a substantial increase in the macroH2A1 content of liver as mice mature from newborns to young adults (Fig. 5). Our results indicate that this increase contributes to the down-regulation of specific genes that influence the metabolic state of the liver. The increase of macroH2A1.1 during this period is especially marked, suggesting that it may be important for these effects. We have observed a similar developmental change in macroH2A1 composition in rat liver and kidney (25), suggesting that this may be an evolutionarily conserved mechanism used in a variety of tissues to adapt gene expression to different functional states.

Why is our list of genes that have altered expression levels in a *macroH2A1* knockout short, when macroH2A1 histones are widely distributed in the chromatin? The microarray that we used was designed to examine the expression of all well-described genes as of 2002. Some genes were likely missed due to technical limitations of the arrays or technical problems with our analyses. We believe that genes were missed due to the relatively small effects of the knockout on the level of expression. Normal variation in gene expression or technical variations in our experiments will confound the detection of genes with small changes.

Most of the macroH2A may be involved in silencing regions of the genome, such as the inactive X chromosome, that are controlled by multiple repressive mechanisms. Detecting the effects of a *macroH2A* knockout on many of these regions may require special treatments and single-cell assays, such as those used for detecting X reactivation in *macroH2A1* knockdown cells (15). A recent study showed that a knockdown of macroH2A1 produced a several-hundredfold increase in IL-8

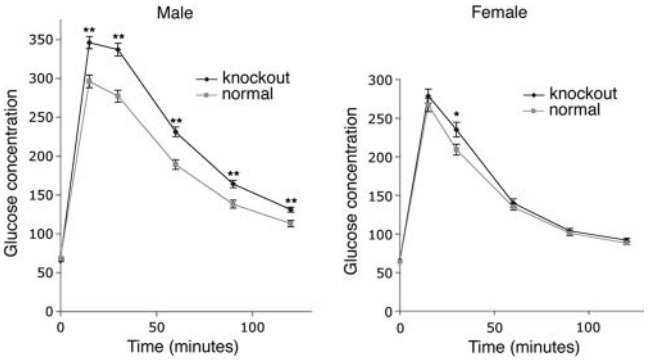

FIG. 6. Glucose tolerance is altered in *macroH2A1* knockout mice. Mice were fasted overnight and injected with 2 g glucose/kg of body weight intraperitoneally, and blood glucose concentrations were measured at 0, 15, 30, 60, 90, and 120 min. The error bars indicate the standard errors of the means. *, $P < 0.05$ (two-tailed t test); **, $P < 0.001$ (two-tailed t test). Numbers of mice: 63 normal males, 49 knockout males, 44 normal females, and 47 knockout females.

expression in a cultured human lymphoid cell line (2). We were not able to examine whether *macroH2A1* is essential for silencing IL-8 in mouse B cells, because mice do not have an IL-8 gene or any obvious homologue. Our gene expression analyses and the mild phenotype of *macroH2A1* knockout mice suggest that dramatic derepression of genes is rare in *macroH2A1* knockout mice. While our microarray analysis did not identify any genes showing dramatic derepression, we have detected significant derepression of specific endogenous retroviruses in *macroH2A1* knockout mice (unpublished data). Overall, we believe that there is good evidence that macroH2A1 nucleosomes contribute to maintaining gene silencing in many regions of the genome. Our current study indicates that macroH2A function is not restricted to suppressing inappropriate or unwanted gene expression but also includes fine tuning the expression of specific genes.

ACKNOWLEDGMENTS

We thank Austin Smith for providing the plasmid pGTiresbgeo, Don Baldwin and John Tobias for assistance with the microarrays, Katherine McKeown for work on the cDNA subtraction experiment, Linden Craig for assistance with histopathology, Mitchell Lazar and Rexford Ahima for suggestions related to metabolic tests, Lionel Larue for assistance with the knockout, Rachel Weinstein for assistance with statistical analyses, and Mike Atchison and Narayan Avadhani for comments on the manuscript.

This work was supported by Public Health Service grant GM49351 from the National Institute of General Medical Sciences.

REFERENCES

1. **Abbott, D. W., M. Laszczak, J. D. Lewis, H. Su, S. C. Moore, M. Hills, S. Dimitrov, and J. Ausio.** 2004. Structural characterization of macroH2A containing chromatin. Biochemistry **43:**1352–1359.
2. **Agelopoulos, M., and D. Thanos.** 2006. Epigenetic determination of a cell-specific gene expression program by ATF-2 and the histone variant macroH2A. EMBO J. **25:**4843–4853.
3. **Allen, M. D., A. M. Buckle, S. C. Cordell, J. Lowe, and M. Bycroft.** 2003. The crystal structure of AF1521 a protein from Archaeoglobus fulgidus with homology to the non-histone domain of macroH2A. J. Mol. Biol. **330:**503–511.
4. **Chadwick, B. P., and H. F. Willard.** 2001. Histone H2A variants and the inactive X chromosome: identification of a second macroH2A variant. Hum. Mol. Genet. **10:**1101–1113.
5. **Changolkar, L. N., and J. R. Pehrson.** 2006. macroH2A1 histone variants are depleted on active genes but concentrated on the inactive X chromosome. Mol. Cell. Biol. **26:**4410–4420.
6. **Costanzi, C., and J. R. Pehrson.** 1998. Histone macroH2A1 is concentrated in the inactive X chromosome of female mammals. Nature **393:**599–601.
7. **Costanzi, C., and J. R. Pehrson.** 2001. MACROH2A2, a new member of the MACROH2A core histone family. J. Biol. Chem. **276:**21776–21784.
8. **Costanzi, C., P. Stein, D. M. Worrad, R. M. Schultz, and J. R. Pehrson.** 2000. Histone macroH2A1 is concentrated in the inactive X chromosome of female preimplantation embryos. Development **127:**2283–2289.
9. **Csankovszki, G., A. Nagy, and R. Jaenisch.** 2001. Synergism of Xist RNA, DNA methylation, and histone hypoacetylation in maintaining X chromosome inactivation. J. Cell Biol. **153:**773–783.
10. **Doyen, C. M., W. An, D. Angelov, V. Bondarenko, F. Mietton, V. M. Studitsky, A. Hamiche, R. G. Roeder, P. Bouvet, and S. Dimitrov.** 2006. Mechanism of polymerase II transcription repression by the histone variant macroH2A. Mol. Cell. Biol. **26:**1156–1164.
11. **Grigoryev, S. A., T. Nikitina, J. R. Pehrson, P. B. Singh, and C. L. Woodcock.** 2004. Dynamic relocation of epigenetic chromatin markers reveals an active role of constitutive heterochromatin in the transition from proliferation to quiescence. J. Cell Sci. **117:**6153–6162.
12. **Gu, H., Y. R. Zou, and K. Rajewsky.** 1993. Independent control of immunoglobulin switch recombination at individual switch regions evidenced through Cre-loxP-mediated gene targeting. Cell **73:**1155–1164.
13. **Halleck, M. S., J. J. Lawler, S. Blackshaw, L. Gao, P. Nagarajan, C. Hacker, S. Pyle, J. T. Newman, Y. Nakanishi, H. Ando, D. Weinstock, P. Williamson, and R. A. Schlegel.** 1999. Differential expression of putative transbilayer amphipath transporters. Physiol. Genomics **1:**139–150.
14. **He, W., F. J.-P. Miao, D. C.-H. Lin, R. T. Schwandner, Z. Wang, J. Gao, J.-L. Chen, H. Tian, and L. Ling.** 2004. Citric acid cycle intermediates as ligands for orphan G-protein-coupled receptors. Nature **429:**188–193.
15. **Hernandez-Munoz, I., A. H. Lund, P. van der Stoop, E. Boutsma, I. Muijrers, E. Verhoeven, D. A. Nusinow, B. Panning, Y. Marahrens, and M. V. Lohuizen.** 2005. Stable X chromosome inactivation involves the PRC1 Polycomb complex and requires histone MACROH2A1 and the CULLIN3/SPOP ubiquitin E3 ligase. Proc. Natl. Acad. Sci. USA **102:**7635–7640.
16. **Hoyer-Fender, S., C. Costanzi, and J. R. Pehrson.** 2000. Histone macroH2A1.2 is concentrated in the XY-body by the early pachytene stage of spermatogenesis. Exp. Cell Res. **258:**254–260.
17. **Karras, G. I., G. Kustatscher, H. R. Buhecha, M. D. Allen, C. Pugieux, F. Sait, M. Bycroft, and A. G. Ladurner.** 2005. The *macro* domain is an ADP-ribose binding module. EMBO J. **24:**1911–1920.
18. **Kim, J. K., J. J. Fillmore, Y. Chen, C. Yu, I. K. Moore, M. Pypaert, E. P. Lutz, Y. Kako, W. Velez-Carrasco, I. J. Goldberg, J. L. Breslow, and G. I. Shulman.** 2001. Tissue-specific overexpression of lipoprotein lipase causes tissue-specific insulin resistance. Proc. Natl. Acad. Sci. USA **98:**7522–7527.
19. **Kraegen, E. W., P. W. Clark, A. B. Jenkins, E. A. Daley, D. J. Chisholm, and L. H. Storlien.** 1991. Development of muscle insulin resistance after liver insulin resistance in high-fat-fed rats. Diabetes **40:**1397–1403.
20. **Laping, N. J., B. A. Olson, and Y. Zhu.** 2001. Identification of a novel nuclear guanosine triphosphate-binding protein differentially expressed in renal disease. J. Am. Soc. Nephrol. **12:**883–890.
21. **Marahrens, Y., B. Panning, J. Dausman, W. Strauss, and R. Jaenisch.** 1997. Xist-deficient mice are defective in dosage compensation but not spermatogenesis. Genes Dev. **11:**156–166.
22. **Mountford, P., B. Zevnik, A. Duwel, J. Nichols, M. Li, C. Dani, M. Robertson, I. Chambers, and A. Smith.** 1994. Dicistronic targeting constructs: reporters and modifiers of mammalian gene expression. Proc. Natl. Acad. Sci. USA **91:**4303–4307.
23. **Ntambi, J. M.** 1999. Regulation of stearoyl-CoA desaturase by polyunsaturated fatty acids and cholesterol. J. Lipid Res. **40:**1549–1558.
24. **Pehrson, J. R.** 2004. Core histone variants, p. 181–204. *In* J. Zlatanova and S. H. Leuba (ed.), Chromatin structure and dynamics: state of the art, vol. 29. Elsevier, Amsterdam, The Netherlands.
25. **Pehrson, J. R., C. Costanzi, and C. Dharia.** 1997. Developmental and tissue expression patterns of histone macroH2A1 subtypes. J. Cell. Biochem. **65:**107–113.
26. **Pehrson, J. R., and V. A. Fried.** 1992. MacroH2A, a core histone containing a large nonhistone region. Science **257:**1398–1400.
27. **Pehrson, J. R., and R. N. Fuji.** 1998. Evolutionary conservation of macroH2A subtypes and domains. Nucleic Acids Res. **26:**2837–2842.
28. **Pohl, J., A. Ring, U. Korkmaz, R. Ehehalt, and W. Stremmel.** 2005. FAT/CD36-mediated long-chain fatty acid uptake in adipocytes requires plasma membrane rafts. Mol. Biol. Cell **16:**24–31.
29. **Preiss-Landl, K., R. Zimmermann, G. Hammerle, and R. Zechner.** 2002. Lipoprotein lipase: the regulation of tissue specific expression and its role in lipid and energy metabolism. Curr. Opin. Lipidol. **13:**471–481.
30. **Rasmussen, T. P., T. Huang, M. A. Mastrangelo, J. Loring, B. Panning, and R. Jaenisch.** 1999. Messenger RNAs encoding mouse histone macroH2A1 isoforms are expressed at similar levels in male and female cells and result from alternative splicing. Nucleic Acids Res. **27:**3685–3689.
31. **Schussler, G. C.** 2000. The thyroxine-binding proteins. Thyroid **10:**141–149.
32. **Tusher, V. G., R. Tibshirani, and G. Chu.** 2001. Significance analysis of microarrays applied to the ionizing radiation response. Proc. Natl. Acad. Sci. USA **98:**5116–5121.
33. **Yeh, S., M. Y. Tsai, Q. Xu, X. M. Mu, H. Lardy, K. E. Huang, H. Lin, S. D. Yeh, S. Altuwaijri, X. Zhou, L. Xing, B. F. Boyce, M. C. Hung, S. Zhang, L. Gan, and C. Chang.** 2002. Generation and characterization of androgen receptor knockout (ARKO) mice: an in vivo model for the study of androgen functions in selective tissues. Proc. Natl. Acad. Sci. USA **99:**13498–13503.
34. **Zaragonza-Hermans, N., and J. P. Felber.** 1971. Studies of the metabolic effect induced in the rat by a high fat diet. II. Disposal of orally administered (14C)-glucose. Horm. Metab. Res. **4:**25–30.
35. **Zhang, J. S., L. Wang, H. Huang, M. Nelson, and D. I. Smith.** 2001. Keratin 23 (K23), a novel acidic keratin, is highly induced by histone deacetylase inhibitors during differentiation of pancreatic cancer cells. Genes Chromosomes Cancer **30:**123–135.
36. **Zhang, R., M. V. Poustovoitov, X. Ye, H. A. Santos, W. Chen, S. M. Daganzo, J. P. Erzberger, I. G. Serebriiskii, A. A. Canutescu, R. L. Dunbrack, J. R. Pehrson, J. M. Berger, P. D. Kaufman, and P. D. Adams.** 2005. Formation of MacroH2A-containing senescence-associated heterochromatin foci and senescence driven by ASF1a and HIRA. Dev. Cell **8:**19–30.
37. **Zhu, Q., G. W. Anderson, G. T. Mucha, E. J. Parks, J. K. Metkowski, and C. N. Mariash.** 2005. The Spot 14 protein is required for de novo lipid synthesis in the lactating mammary gland. Endocrinology **146:**3343–3350.